Journal of Biomolecular NMR, **21:** 281–284, 2001.
KLUWER/ESCOM

Letter to the Editor: NMR structure of human fibronectin EDA

Tatsuya Niimi*, Masanori Osawa, Noboru Yamaji, Kunio Yasunaga, Hitoshi Sakashita, Toshiyasu Mase, Akihiro Tanaka & Shigeo Fujita
Institute for Drug Discovery Research, Yamanouchi Pharmaceutical Co., Ltd., 21, Miyukigaoka, Tsukuba-shi, Ibaraki 305-8585, Japan

Received 23 June 2001; Accepted 27 August 2001

Key words: EDA, fibronectin, folding, tertiary structure, triple resonance NMR

Biological context

Fibronectin is a large multifunctional glycoprotein involved in cell adhesion, cell migration, wound healing and the regulation of cell growth. Fibronectin is a modular protein composed of three different modules termed types I–III. These independently-folded modules provide multiple binding sites for cell receptors of the integrin families and for other extracellular matrix (ECM) proteins. There are several variants, all of which originate from alternative splicing of FNIII domains (EDA, EDB and IIICS). Fibronectin containing EDA is highly expressed during embryogenesis, but only slightly expressed in adult tissue except on special pathological conditions such as wound healing, liver fibrosis, glomerulosclerosis, vascular neoinitima and cardiac transplantation. The biological function of EDA itself, however, is still poorly understood. Here, we present the tertiary structure of the human EDA (hEDA) in solution. Its dynamic conformational property will also be discussed.

Methods and results

DNA fragment coding hEDA was obtained by PCR reactions of cDNA prepared from human liver mRNA. Recombinant hEDA was expressed in *E. coli* BL21(DE3). Purified samples were concentrated to 1–2 mM in a $^2H_2O/^1H_2O$ (1:9) solution of 20 mM sodium phosphate (pH 7.0) and 50 mM NaCl or 400 mM Na_2SO_4. All NMR spectra were recorded on a Bruker AMX-600. ^1H, ^{13}C and ^{15}N assignments were carried out by using ^{15}N-^1H HSQC, HNCA, HN(CO)CA, HNCO, HNCACB, CBCA(CO)NH, HBHA(CBCACO)NH, H(CCO)NH, C(CO)NH, HCCH-TOCSY and ^{13}C-edited NOESY-HSQC. The stereospecific assignment of the valine and leucine methyl groups were obtained by biosynthetically directed fractional 10% ^{13}C labeling. All data were processed by nmrPipe (Delaglio, 1993) and data analysis was assisted by the software Pipp (Garrett et al., 1991). Interproton restraints for the structure calculations were obtained from ^{13}C-edited NOESY-HSQC and ^{15}N-edited NOESY-HSQC with 50 ms mixing time. Slowly exchanging amide protons were identified by monitoring the series of ^{15}N-^1H HSQC spectra recorded at different time points. The coupling constants $^3J_{HN-H\alpha}$ were measured from the HNHA experiment. The ϕ and ψ dihedral angle restraints were derived from the $^3J_{HN-H\alpha}$ coupling constants and chemical shifts indices. The structures were calculated using the YASAP protocol (Nilges et al., 1988) within X-PLOR (Brunger, 1992).

The boundaries of hEDA were originally chosen in a reference to other FNIII sequences to encode a 90-residue domain (hEDA(1-90)). The ^{15}N-^1H HSQC spectrum of hEDA(1-90) at 20 °C in 50 mM sodium phosphate buffer (pH 7.0) containing 50 mM NaCl showed the expected number of resonances for a protein of 90 amino acid residues, having chemical shifts typical of a random coil (7.8–8.5 ppm) (Figure 1a). This suggests that the isolated hEDA(1-90) is unfolded, unlike the other single FNIII domains such as fibronectin 10th FNIII repeat (fnFNIII10), EDB and tenascin third FNIII repeat (tnFNIII3) (Main et al., 1992; Hamill et al., 1998; Fattorusso et al., 1999). The hEDA extended by four residues derived from the neighboring fnFNIII12 sequence at the C-terminus (hEDA(1-94)) exhibited twice the number of expected peaks for a protein of 90 amino acid residues in the

*To whom correspondence should be addressed. E-mail: niimi@yamanouchi.co.jp

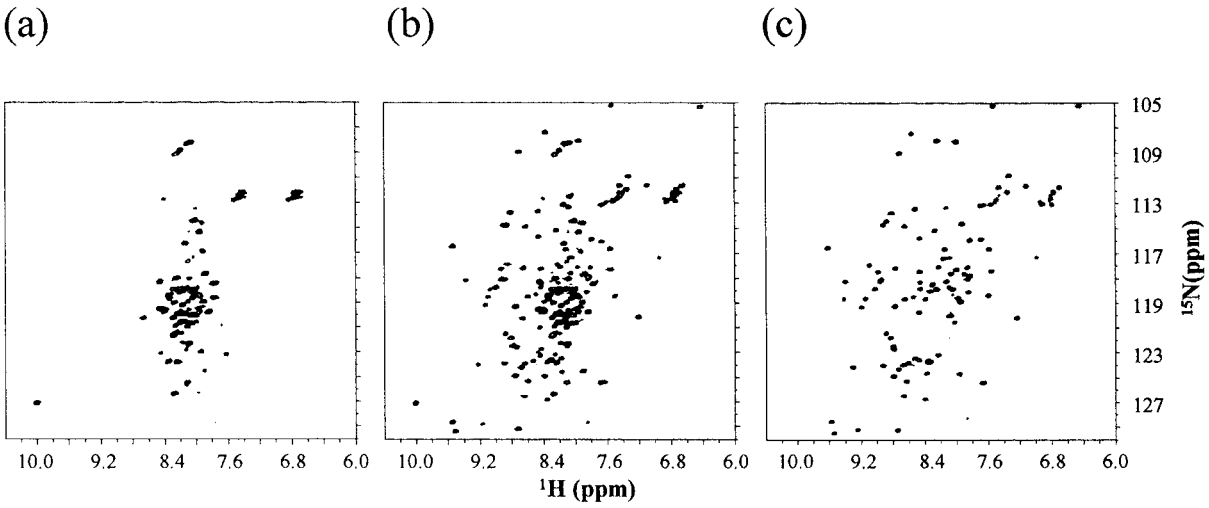

Figure 1. ^{1}H-^{15}N HSQC spectra of two hEDA species in two different conditions. (a) hEDA(1-90) in 50 mM NaCl. (b) hEDA(1-94) in 50 mM NaCl. (c) hEDA(1-94) in 400 mM Na_2 SO_4. All spectra were recorded at 20 °C in 20 mM sodium phosphate buffer (pH 7.0).

^{15}N-^{1}H HSQC spectrum (Figure 1b), half of which had a chemical shift dispersion characteristic of the folded protein. Raising the temperature caused a gradual reduction in the intensity of the cross peaks outside the random-coil region, and these peaks mostly disappeared at 37 °C at which numerous other FNIII domains are stable (data not shown). Because this thermal transition was reversible, it is likely that the slow conformational exchange on the NMR time scale is present between the folded and unfolded states of the hEDA. The further addition of 4–12 residues to the C-terminus did not affect the equilibrium between the folded and the unfolded state of hEDA(1-94) (data not shown).

The resonances of the unfolded state disappeared upon addition of 400 mM Na_2SO_4 (Figure 1c). The overall structure in the presence of Na_2SO_4 and that of the folded state in the absence of Na_2SO_4 appeared to be same, because the backbone ^{15}N chemical shifts were nearly identical. Thus, the following structure determination was carried out for hEDA(1-94) in the presence of Na_2SO_4 at 20 °C.

Sequence-specific assignments of the backbone resonances were obtained except for N1 at the N-terminus and D78-M79. For the side-chain assignments, the Cγ, Cδ, Hγ and Hδ resonances of several proline residues and the indole CH signals of H44 and H76 were unassigned. The aromatic CH signals of Y32 were not observed probably due to flipping of the aromatic ring, in a fashion similar to fnFNIII9 and fnFNIII10 (Copie et al., 1998). The chemical shift values of ^{1}H, ^{13}C and ^{15}N resonances were deposited in the BioMagResBank (accession number BMRB-5027).

The secondary structure of hEDA(1-94) was determined on the basis of the NOE data, $^{1}H/^{2}H$ exchange data, $^{3}J_{HN-H\alpha}$ coupling constants data and chemical shift index. The relative locations of the β-strands were determined from the long-range NOEs between the individual β-strands. As anticipated from the sequence alignment with other fnFNIII domains (Dickinson et al., 1994), hEDA(1-94) is composed of seven β-strands (from βA to βG) where conserved amino acids among the fnFNIII domains are found at approximately analogous positions. The only exception is the position of βD. The counterpart of Y36 is H44 but not E45 which had been predicted from the sequence alignment. Furthermore, βD stretches from G42 to L46 and shifts upward by three residues from the predicated secondary structure, which results in the short CD loop consisting of 3 residues (usually 6–8 residues in other fnFNIII domains) and the long DE loop consisting of 9 residues (usually 5–6 residues). This is probably because the presence of P48 perturbs the βD strand formation at the authentic position. The long DE loop contains the acidic-residue cluster (D51, E53, E54 and D55). This is characteristic of hEDA, because the corresponding loop in other fnFNIII domains has only one acidic residue at most.

The three-dimensional structure of hEDA(1-94) was determined from the total 1340 experimental restraints (Table 1). The structure statistics for 20 low

Table 1. Summary of Restraints for hEDA(1-94) in structure calculations

Type	Number of restraints
All	1340
Distance constraints	1289
Intraresidue (i = j)	435
Sequential (|i−j|=1)	332
Short range (|i−j|<5)	87
Long range (|i−j| ≥ 5)	381
Hydrogen bond	54
Dihedral restraints	51
ϕ angle	33
ψ angle	18

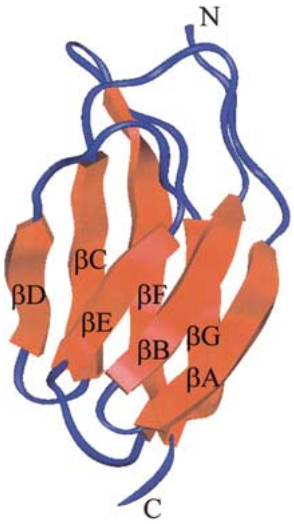

Figure 2. The overall fold of the energy-minimized average structure of hEDA(1-94). The seven β-sheets are labeled (βA-βG).

energy NMR structures are summarized in Table 2. hEDA(1-94) adopts the classical FNIII fold consisting of two antiparallel β-sheets that form a β-sandwich (Figure 2). The two β sheets enclose a well-defined hydrophobic core of 22 amino acids: L8, F10, V13, I18, I20, W22, P25, V29, Y32, V34, Y36, L46, A57, L59, L62, Y68, V70, V72, A74, L84, G86 and T90 (Figure 3). The root mean-square deviations in backbone atoms in β-sheet regions of hEDA(1-94) relative to other FNIII domains are 0.94 Å, 1.15 Å, 1.11 Å and 1.71 Å for fnFNIII8, fnFNIII9, fnFNIII10 and tnFNIII3, respectively (PDB ID code: 1FNF and 1TEN). The atom coordinates have been deposited in the Protein Data Bank (PDB ID code 1J8K).

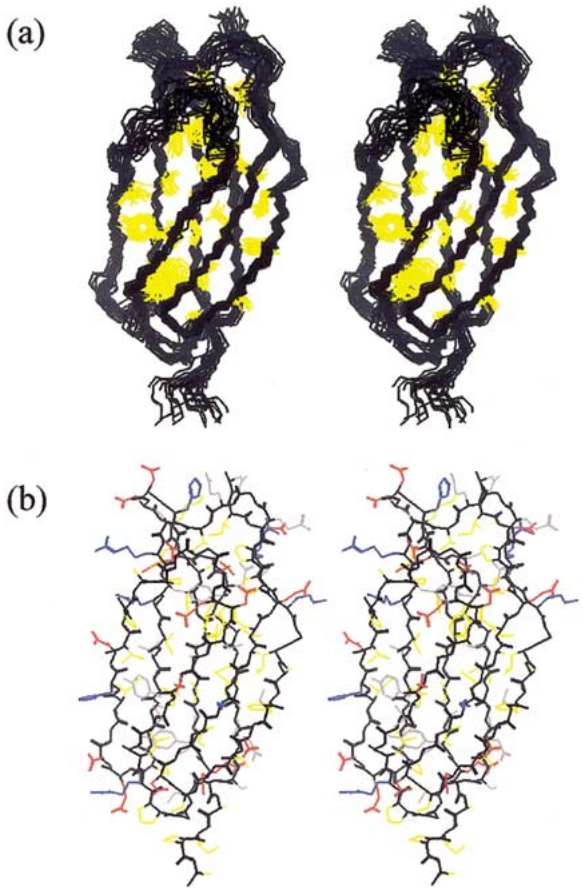

Figure 3. Different stereorepresentations of hEDA(1-94). (a) Superposition of the side-chains forming the hydrophobic core together with the backbone atoms (N, Cα, and C') of the selected 20 NMR-derived structures of hEDA(1-94). Tertiary structures of hEDA(1-94) were superimposed onto the energy-minimized average structure using β-sheets regions. The side-chains forming the hydrophobic core are indicated by yellow. (b) Heavy-atom display of the energy-minimized average structure. The following color code was used: black, backbone; yellow, hydrophobic side-chains; gray, polar side-chains; blue, positively charged side-chains; red, negatively charged side.

Discussion and conclusion

The FNIII domain is generally a stable module. Most FNIII domains have a melting temperature higher than 60 °C at neutral pH. In contrast, isolated hEDA(1-94) is mostly unfolded at 37 °C and exists in dynamic equilibrium between the folded and the unfolded states at 20 °C on the physiological condition. Furthermore, hEDA(1-90) became unfolded by the removal of the four C-terminal residues. This suggests that hEDA can be easily transformed to the unfolded state as a result of mechanical stress on the molecule through

Table 2. Structure statistics of hEDA(1-94) NMR structures

	{SA}		<SA>r
(A) X-PLOR energies (kcal/mol)			
E_{total}	168	± 8	163
E_{bond}	8.8	± 0.7	8.7
E_{angle}	117	± 4	114
$E_{improper}$	18	± 1	17
E_{vdw}	7.4	± 1.8	6.7
E_{noe}	17	± 3	18
E_{cdih}	0.02	± 0.03	0.02
(B) r.m.s.d from idealized geometry			
Bonds (Å)	0.004	± 0.001	0.004
Angles (deg)	0.54	± 0.002	0.54
Impropers (deg)	0.40	± 0.004	0.40
(C) r.m.s.d from experimental restraints			
NOE (Å)	0.016	± 0.002	0.017
dihedral angle (deg)	0.06	± 0.06	0.07
(D) r.m.s.d to mean structure (Å)			
All non-H atoms in all regions	1.34	± 0.09	
All non-H atoms in β-sheet regions	0.93	± 0.08	
Backbone atoms in all regions	0.89	± 0.10	
Backbone atoms in β-sheet regions	0.51	± 0.06	

{SA} refers to the final 20 simulated annealing structures; <SA>r refers to mean regularized structure obtained from superposition of core backbone atoms of 20 NMR structures followed by restrained regularization of the mean structure. The 20 structures have no NOE violations greater than 0.3 Å and no dihedral angle restraint violations > 1.0 deg.

E_{noe} and E_{cdih}were calculated using force constants of 50 kcal mol^{-1} $Å^{-2}$ and 200 kcal mol^{-1} rad^{-2}, respectively.

E_{vdw} was calculated using a final value of 4.0 kcal mol^{-1} $Å^{-4}$ with the van der Waals hard sphere radii set to 0.75 times those in the parameter set PARALLHDG supplied with X-PLOR.

an external force such as cytoskeletal machinery. Recent studies of titin and tenascin show that an external pulling force on the entire protein results in the consecutive unfolding of the individual FNIII domains in an all-or-none fashion (for a review, see Zhu et al., 2000). These data indicate that the folding/unfolding reaction may contribute to extensibility or elasticity of the FNIII repeat-containing molecules and regulate the ligand-binding activity as a recognition switch. Several FNIII domains of fibronectin have been elucidated to contain cryptic sites that are recognized by other fibronectin domains, becoming exposed only after at least a partial unfolding (Hocking et al., 1996; Litvinovich et al., 1998).

There are two possible mechanisms of how EDA may function in the whole molecule. The first possibility is that the insertion of EDA induces a local and/or global conformational change in fibronectin (Manabe et al., 1997; Johnson et al., 1999), which could cause stabilization or destabilization of the individual FNIII domains. The second possibility is that EDA itself binds to a cell-surface receptor and regulates the matrix assembly or interaction between the fibronectin and other proteins. Although the receptor of EDA remains unidentified, the presence of the receptor has been suggested by the study of the recombinant EDA or monoclonal antibody recognizing EDA (Jarnagin et al., 1994; Xia and Culp, 1995; Serini et al., 1998). In either case, this conformational equilibrium may play a key role in the physiological function of EDA. The detailed characterization will provide useful information about the unique functional role of EDA.

References

Brunger, A.T. (1992) *X-PLOR Version 3.1. A System for X-ray Crystallography and NMR*, Yale University Press, New Haven, CT.

Copie, V., Tomita, Y., Akiyama, S.K., Aota, S., Yamada, K.M., Venable, R.M., Pastor, R.W., Krueger, S. and Torchia, D.A. (1998) *J. Mol. Biol.*, **277,** 663–682.

Delaglio, F. (1993) *NMRPipe System of Software*, National Institutes of Health, Bethesda, MD.

Dickinson, C.D., Veerapandian, B., Dai, X.P., Hamlin, R.C., Xuong, N.H., Ruoslahti, E. and Ely, K.R. (1994) *J. Mol. Biol.*, **236,** 1079–1092.

Fattorusso, R., Pellecchia, M., Viti, F., Neri, P., Neri, D. and Wüthrich, K. (1999) *Structure*, **7**, 381–390.

Garrett, D.S., Powers, R., Gronenborn, A.M. and Clore, G.M. (1991) *J. Magn. Reson.*, **95**, 214–220.

Goll, C.M., Pastore, A. and Nilges, M. (1998) *Structure*, **6**, 1291–1302.

Hamill, S.J., Meekhof, A.E. and Clarke, J. (1998) *Biochemistry*, **37**, 8071–8079.

Hocking, D.C., Smith, R.K. and McKeown-Longo P.J. (1996) *J. Cell Biol.*, **133**, 431–444.

Jarnagin, W.R., Rockey, D.C., Koteliansky, V.E., Wang, S.S. and Bissell, D.M. (1994) *J. Cell. Biol.*, **127**, 2037–2048.

Johnson, K.J., Sage, H., Briscoe, G. and Erickson, H.P. (1999) *J. Biol. Chem.*, **274**, 15473–15479.

Litvinovich, S.V., Brew, S.A., Aota, S., Akiyama, S.K., Haudenschild, C. and Ingham, K.C. (1998) *J. Mol. Biol.*, **280**, 245–258.

Main, A.L., Harvey, T.S., Baron, M., Boyd, J. and Campbell, I.D. (1992) *Cell*, **71**, 671–678.

Manabe, R., Ohe, N., Maeda, T., Fukuda, T. and Sekiguchi, K. (1997) *J. Cell. Biol.*, **139**, 295–307.

Nilges, M., Gronenborn, A.M., Brunger, A.T. and Clore, G.M. (1988) *Protein Eng.*, **2**, 27–38.

Serini, G., Bochaton-Piallat, M.L., Ropraz, P., Geinoz, A., Borsi, L., Zardi, L. and Gabbiani, G. (1998) *J. Cell. Biol.*, **142**, 873–881.

Xia, P. and Culp, L.A. (1995) *Exp. Cell. Res.*, **217**, 517–527.

Zhu, C., Bao, G. and Wang, N. (2000) *Annu. Rev. Biomed. Engr.*, **2**, 189–226.